Sexual Medicine, 2025, **13**, qfaf007
https://doi.org/10.1093/sexmed/qfaf007
Original Research

The conserved molecular mechanism of erectile dysfunction in type 2 diabetes rats and mice by cross-species transcriptomic comparisons

Ming Xiao, PhD[1,2], Huanqing Zeng, MSc[1,2], Yanghua Xu, PhD[1,2], Jiarong Xu, PhD[1,2], Xiaoli Tan, MSc[1,2], Yuxin Tang, PhD[1,2,*]

[1]Department of Urology, The Fifth Affiliated Hospital of Sun Yat-Sen University, Zhuhai, Guangdong Province 519000, China
[2]Guangdong Provincial Key Laboratory of Biomedical Imaging, The Fifth Affiliated Hospital of Sun Yat-Sen University, Zhuhai, Guangdong Province 519000, China
*Corresponding author: Department of Urology, The Fifth Affiliated Hospital of Sun Yat-Sen University, Xiangzhou District, Zhuhai, Guangdong Province 519000, China. Email: tangyx36@mail.sysu.edu.cn

Abstract

Background: The poor clinical situation of type 2 diabetes-induced erectile dysfunction (T2DMED) creates an urgent need for new therapeutic targets.
Aim: To reveal the conserved molecular mechanism of T2DMED across species.
Methods: T2DMED rat and mouse models were constructed to extract mRNA from corpus cavernosum for high-throughput sequencing. The differentially expressed genes (DEGs) were analyzed and the Kyoto Encyclopedia of Genes and Genomes (KEGG), Gene Ontology (GO), and Protein–Protein Interaction Networks were performed by bioinformatics methods. Immunohistochemistry, immunofluorescence, hematoxylin-eosin and Masson staining were used for subsequent verification.
Outcomes: Cross-species transcriptomics of T2DMED rats and mice were analyzed and validated.
Results: Gene expression patterns in normal corpus cavernosum of mice and rats showed a strong correlation ($r = 0.75$, $P < 2.2 \times 10^{-16}$), with a total of 15 691 homologous genes identified. In both species, 553 homologous down-regulated DEGs were identified, mainly enriched in pathways related to smooth muscle and mitochondrial functions, as revealed by KEGG and GO analyses. Immunohistochemistry and immunofluorescence confirmed the decreased expression of α-smooth muscle actin and *Uqcr10* in cavernosum tissues of T2DMED mice and rats. Additionally, 239 homologous up-regulated DEGs were identified, which were enriched in the *Wnt* signaling pathway and extracellular matrix composition. Subsequent experiments confirmed increased β-catenin expression and significant collagen accumulation, indicating fibrosis in T2DMED.
Clinical implications: To provide a new direction for improving the erectile ability of patients with T2DMED.
Strengths and limitations: The main strength is that cross-species transcriptomic sequencing has revealed the conserved molecular mechanisms of T2DMED. The main limitation is the lack of further validation in the T2DMED patients.
Conclusions: Cross-species transcriptomic comparisons may offer a novel strategy for uncovering the underlying mechanisms and identifying therapeutic targets for T2DMED.

Keywords: type 2 diabetes mellitus; erectile dysfunction; cross-species transcriptome; mitochondrial function; extracellular matrix.

Introduction

Erectile dysfunction (ED) is a significant organic disorder affecting the male sexual health, which is estimated to reach 322 million worldwide by 2025.[1] Diabetes mellitus, particularly type 2 diabetes (T2DM), is a major risk factor for ED, with the prevalence of diabetes-induced erectile dysfunction (DMED) ranging from 35.8% to 86.1% in various regions.[2] ED is often a precursor to cardiovascular diseases and diabetes, with 12% of diabetic patients presenting with ED as their initial symptom.[3] In contrast to type 1 diabetes, which is primarily caused by autoimmune destruction of pancreatic islet cells, T2DM is largely attributed to long-term unhealthy lifestyle and accounts for the majority of diabetes cases.[4] The incidence of ED in T2DM patients is 1.9 to 4 times higher than in non-diabetic individuals, with onset typically occurring 10 to 15 years earlier.[5,6]

Current treatment strategies for ED, such as glycemic control, do not fully restore normal erectile capacity in T2DM patients, necessitating additional therapeutic approaches.[7] Phosphodiesterase type 5 inhibitors, which improve erectile function by promoting the relaxation of cavernous smooth muscle through the increased levels of cyclic guanosine monophosphate, are considered first-line treatments, but, 44% of DMED patients perceive insufficient improvement.[8] Furthermore, the second-line therapies, such as intracavernous administration and vacuum devices, often lead to undesirable side effects, including penile pain, abnormal erections, and even cavernous fibrosis, with complication ranging from 24% to 61%.[8-10]

Animal models are frequently used in biomedical research to study human physiological and pathological processes. Among these, rat and mouse are the most commonly

Received: October 28, 2024. **Revised:** February 1, 2025. **Accepted:** February 6, 2025

models in DMED research. However, the findings from animal models are not always directly applicable to humans due to inherent interspecies differences.[11] Investigating biological processes that are conserved across species provide an innovative strategy for identifying potential therapeutic targets for DMED.[12,13] In this study, we conducted a comparative transcriptomic analysis of the corpus cavernosum from T2DMED rats and mice to address the question: What are the common pathological changes of penile tissue and molecular mechanisms of ED underlying T2DM?

Materials and methods

Animal model

All animal procedures were approved by the Animal Care and Use Committee of the Fifth Affiliated Hospital of Sun Yat-Sen University (Approval No. 00369) and were performed in strict compliance with NIH guidelines for laboratory animal care and use. The T2DM model was induced using a high-fat diet combined with low-dose streptozotocin, with slight variations between rats and mice.[14,15] Seven-week-old male Sprague–Dawley rats and C57BL/6 N mice were obtained from the Guangdong Provincial Medical Laboratory Animal Center. After 1 week of acclimatization, the animals were randomly divided into control and model groups, with 10 animals in each group. Rats were fed a high-fat diet (45% kcal from fat) for 4 weeks, followed by two intraperitoneal injections of streptozotocin (25 mg/kg) at three-day intervals. Mice received five consecutive intraperitoneal injections of streptozotocin (50 mg/kg). A blood glucose level exceeding 16.7 mmol/L was the diagnostic criterion for diabetes. During the T2DM modeling process, 1 mouse and 2 rats died. After 12 weeks on a high-fat diet, an apomorphine (APO) test was performed to screen for T2DMED. APO (Sigma) was dissolved in saline containing 0.2 mg/mL ascorbic acid and administered via subcutaneous injection into the dorsal neck region at doses of 80 μg/kg for rats and 100 μg/kg for mice. Penile erections were recorded within 30 minutes post-injection, and animals showing no erections during this period were classified as T2DMED. Based on the APO test results, 7 DMED mice and 6 DMED rats were identified. Of these, 3 animals from each group (normal and DMED) were randomly selected for transcriptomic analysis, while the remaining animals were used for histological validation.

cDNA library construction and sequencing

After modeling, the glans, urethra, vascular, and nervous tissues were removed to isolate the penile corpus cavernosum. mRNA was extracted using TRIzol reagent (Invitrogen, Carlsbad, CA, USA) following the instructions. The extraction procedure was similar for both rats and mice: The penis was amputated near the base, and the glans, urethra, and dorsal penile vessels were discarded. The corpus cavernosum tissue was homogenized in liquid nitrogen, and TRIzol was added for 10-15 minutes of incubation on ice. After chloroform extraction, the aqueous phase was collected, and the protein layer was discarded. RNA was precipitated with isopropanol and centrifuged at 12 000 g for 10 minutes at 4°C. The supernatant was discarded, and the RNA pellet was washed twice with 75% ethanol, air-dried, and dissolved in sterile, nuclease-free water. cDNA library construction and sequencing were conducted by Novogene Co. (Beijing, China).

Sequencing data processing

Raw sequencing reads were filtered to obtain clean reads, removing those containing adapters, excessive N bases, or low-quality bases (Qphred ≤ 5 for more than 50% of the sequence). Clean reads were aligned to the reference genome using HISAT2 (v2.0.5). FeatureCounts (v2.0.1) was used to quantify known gene expression levels. Data visualization was performed using ggplot2 (v3.5.1)[16] in R. Gene expression correlations between rat and mouse homologous genes were assessed using Pearson correlation in R (v4.4.0).[17] Differentially expressed genes (DEGs) were identified using DESeq2 (v1.44.0),[18] with multiple hypothesis correction by the Benjamini-Hochberg method. DEGs were defined as $|\log2(\text{fold change})| > 1$ and $\text{p.adj} < 0.05$.

KEGG and GO enrichment analyses

Kyoto Encyclopedia of Genes and Genomes (KEGG) and Gene Ontology (GO) enrichment analyses of DEGs were conducted using clusterProfiler (v4.12.0).[19-21] KEGG was used to identify significantly associated biological pathways, while GO categorized gene functions into biological process (BP), molecular function (MF), and cellular component (CC). The reference gene sets for mouse and rat were "org.Mm.eg.db" and "org.Rn.eg.db," respectively. The Benjamini-Hochberg method was used for multiple testing corrections, with significance set at $\text{p.adj} < 0.05$.

Gene set enrichment analysis

Gene set enrichment analysis (GSEA) was performed to identify pathways enriched among DEGs using clusterProfiler (v4.12.0),[22] with 10 000 permutations. Normalized enrichment scores were used to assess gene set enrichment, with $\text{p.adj} < 0.05$ and $q < 0.25$ considered significant.

PPI network construction

Protein–Protein Interaction (PPI) networks were built by inputting DEGs into the STRING database,[23] and visualization was performed using Cytoscape (v3.10.1).[24] Hub genes were identified using the cytoHubba(v0.1) plug-in, based on neighborhood connectivity (NCC).[25]

Immunofluorescence and immunohistochemistry

For immunofluorescence, sections were blocked with 5% goat serum for 30 minutes at room temperature, then incubated overnight at 4°C with primary antibodies: anti-β-catenin (abclonal, 1:100) and anti-α-smooth muscle actin (α-SMA) (Abcam, 1:100). After washing with tris buffered saline, slides were incubated with fluorescent secondary antibodies and stained with 4',6-DiAmidino-2-PhenylIndole (DAPI) for nuclear visualization.

For immunohistochemistry, antigen retrieval was performed by heating sections in citrate buffer (pH 6.00) at 700 W for 20 minutes. After blocking with 5% goat serum for 30 minutes, sections were incubated with primary antibodies: anti-*Uqcr10* (SAB, 1:50), anti-β-catenin (abclonal, 1:100), and anti-collagen 1 (Servicebio, 1:400), following manufacturer protocols (BOSTER). Sections were then incubated with biotinylated secondary antibodies for 30 minutes, followed by ABC reagent for 30 minutes. DAB substrate (BIOFIVEN) was prepared and applied for 20 minutes, with development monitored under a microscope. After washing, sections were counterstained with hematoxylin, dehydrated, cleared, and

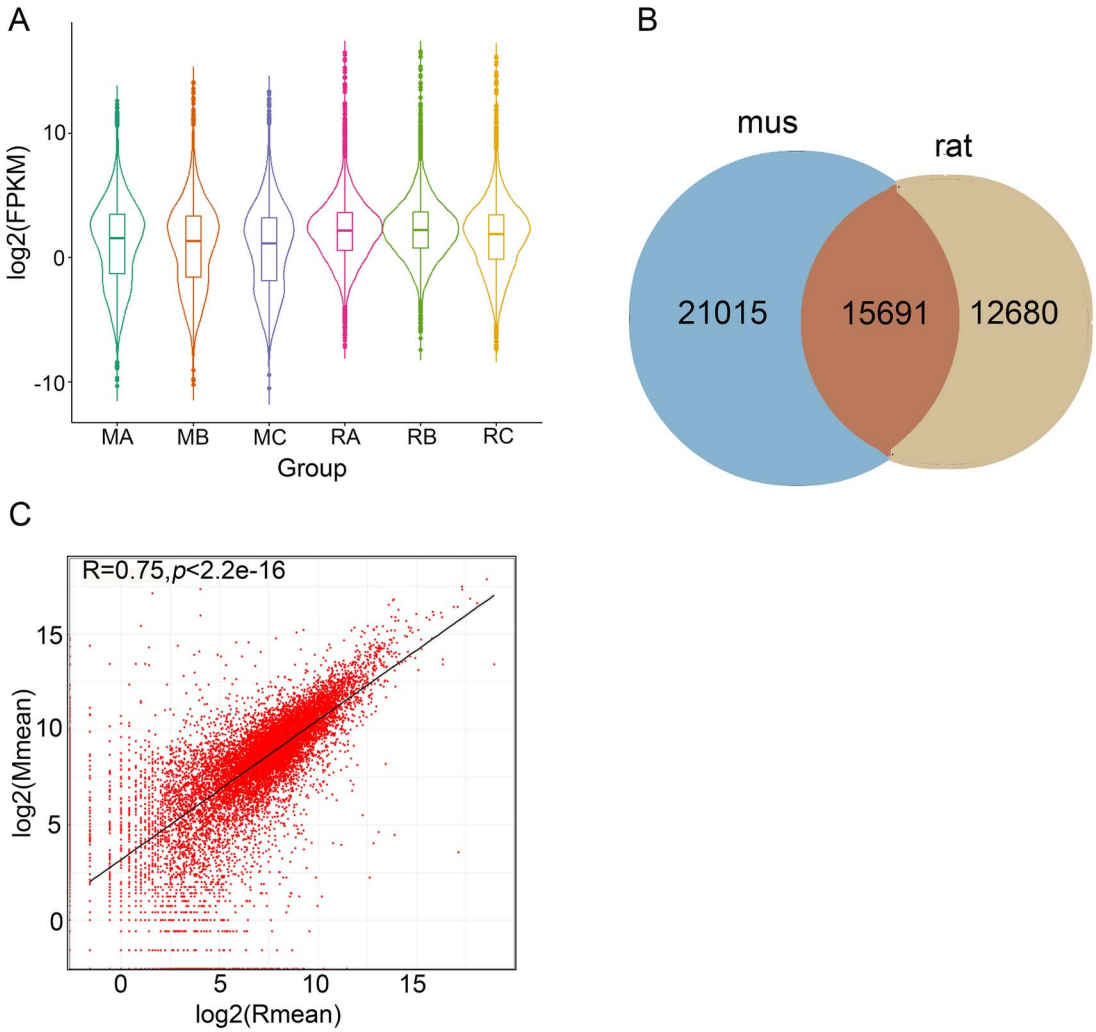

Figure 1. Homologous gene analysis between normal rats and mice. (A) Violin plot showing that the expression of protein-coding genes of corpus cavernosum in normal rats and mice. (B) Venn diagram showing the overlap of homologous genes from corpus cavernosum between normal rats and mice. (C) The correlation of homologous genes of corpus cavernosum between normal rats and mice, analyzed using Pearson correlation analysis. MA, MB, MC: Three samples of corpus cavernosum from the normal mouse group. RA, RB, RC: Three samples of corpus cavernosum from the normal rat group.

mounted. Images were acquired using confocal microscopy (Carl Zeiss AG).

Reactive oxygen species detection

Reactive oxygen species (ROS) detection was performed using a ROS kit (C10422). Fresh penile tissue was frozen, sectioned to 5 μm thickness, and incubated with CellROX™ Deep Red dye (1 μM) and DAPI for 30 minutes at 37°C in a dark, humid environment. Confocal microscopy was used for image acquisition (Carl Zeiss AG).

Hematoxylin-Eosin and Masson staining

For hematoxylin–eosin (HE) staining, slides were stained with hematoxylin for 5 minutes, differentiated in 1% hydrochloric acid alcohol for 1 minute, blued in ammonia water for 1 minute, and stained with eosin for 1 minute. The slides were then dehydrated in graded ethanol and cleared in xylene (5 minutes, thrice) before mounting.

For Masson's trichrome staining, slides were stained with Weigert's hematoxylin for 10 minutes, differentiated in 1% hydrochloric acid alcohol for 1 minute, blued in ammonia water for 1 minute, and stained with Masson's dye for 30 minutes. After eosin staining for 1 minute, slides were dehydrated, cleared in xylene, and mounted. Stained sections were scanned and analyzed using a high-resolution digital pathology system (3DHISTECH).

Statistical analysis

The Shapiro–Wilk test was applied to assess the normality of data distribution. For comparisons between two groups, the Mann–Whitney U test was used for non-normally distributed data, while the Student's t-test was applied for data with a normal distribution. Statistical analyses and visualizations were conducted using GraphPad Prism software (v8), and results are expressed as mean ± standard deviation.

Results

Homologous gene analysis between normal rats and mice

To assess the differences and similarities in gene expression between rat and mouse corpus cavernosum at the

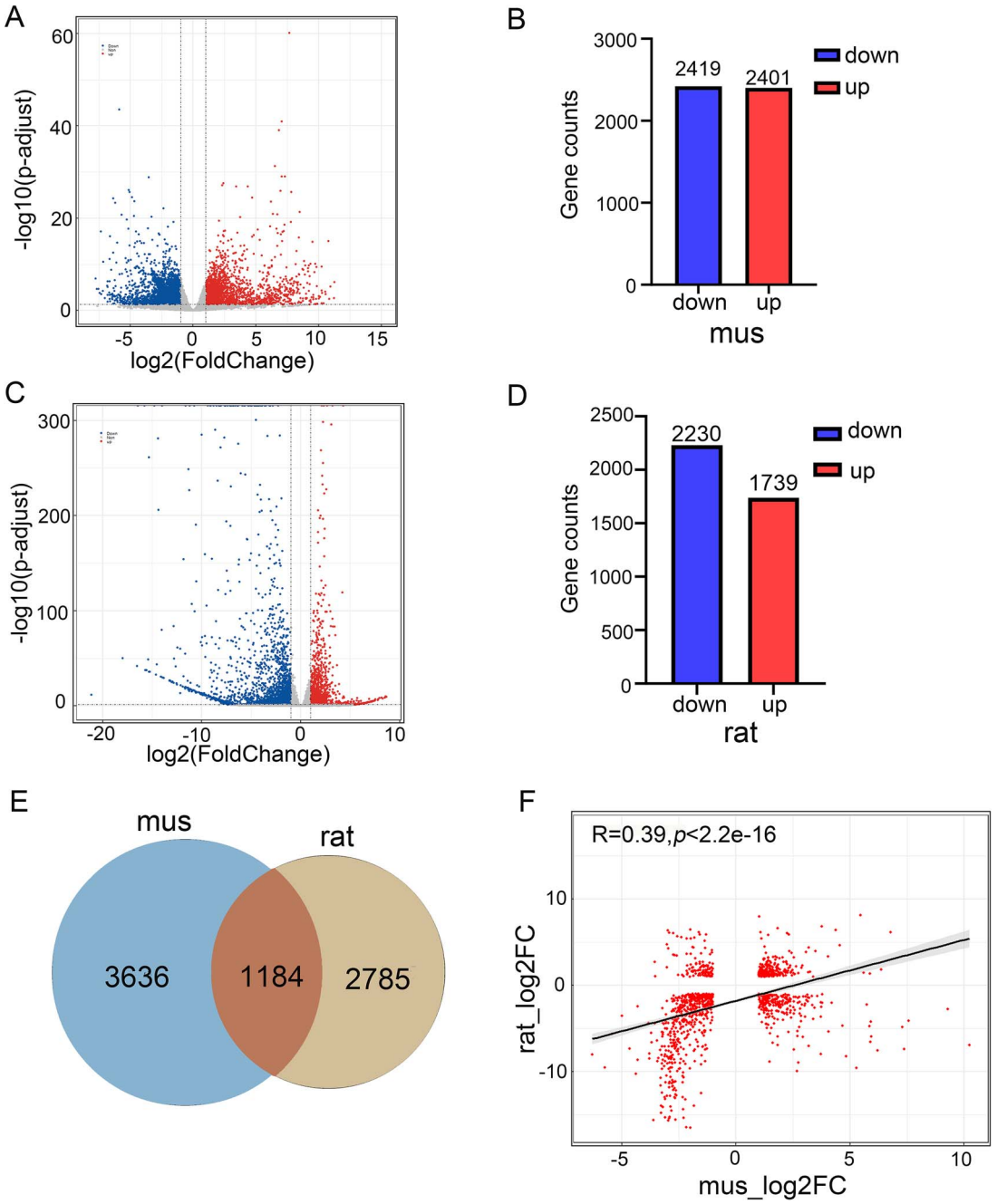

Figure 2. DEGs in T2DMED mice and rats. (A, B) The volcano plot and bar graph of DEGs in T2DMED mice compared to the normal group. (C, D) The volcano plot and bar graph of DEGs in T2DMED rats compared to the normal group. (E) The Venn diagram showing the overlap of DEGs between T2DMED rats and mice. (F) The scatter plot indicating the correlation of common DEGs between the two species. DEGs: differentially expressed genes; mus: mouse; T2DMED: type 2 diabetes-induced erectile dysfunction.

transcriptome level, we collected three normal and T2DMED samples from each species. On average, each mouse sample yielded 30.8 million raw reads, with 94.57% aligning with the reference genome *Mus musculus* (NCBI-GRCm39). Of these, 90.88% mapped to exonic regions, 4.77% to intronic regions, and 4.35% to intergenic regions. Approximately 81.65% (25.15 million reads) were clean reads, which were used for subsequent analysis.

In comparison, each rat sample generated 43.29 million raw reads, with 95.28% aligning to the reference genome *Rattus norvegicus* (Ensembl-Mratbn7). Of these, 89.8% mapped to exonic regions, 5.51% to intronic regions, and 4.69% to intergenic regions. Approximately 95.89% (41.51 million reads) were clean reads used for further analysis.

After the normalization for fragments per kilobase of exon per million fragments mapped, we compared the protein-coding gene expression patterns between normal rats and mice. The expression pattern in mouse corpus cavernosum was relatively uniform, whereas it was more concentrated in rats (Figure 1A). To ensure comparability, we focused on 15 691 homologous genes (Figure 1B). Correlation analysis revealed a high degree of similarity in gene expression between the two species (Pearson correlation, $r = 0.75$, $P < 2.2 \times 10^{-16}$) (Figure 1C).

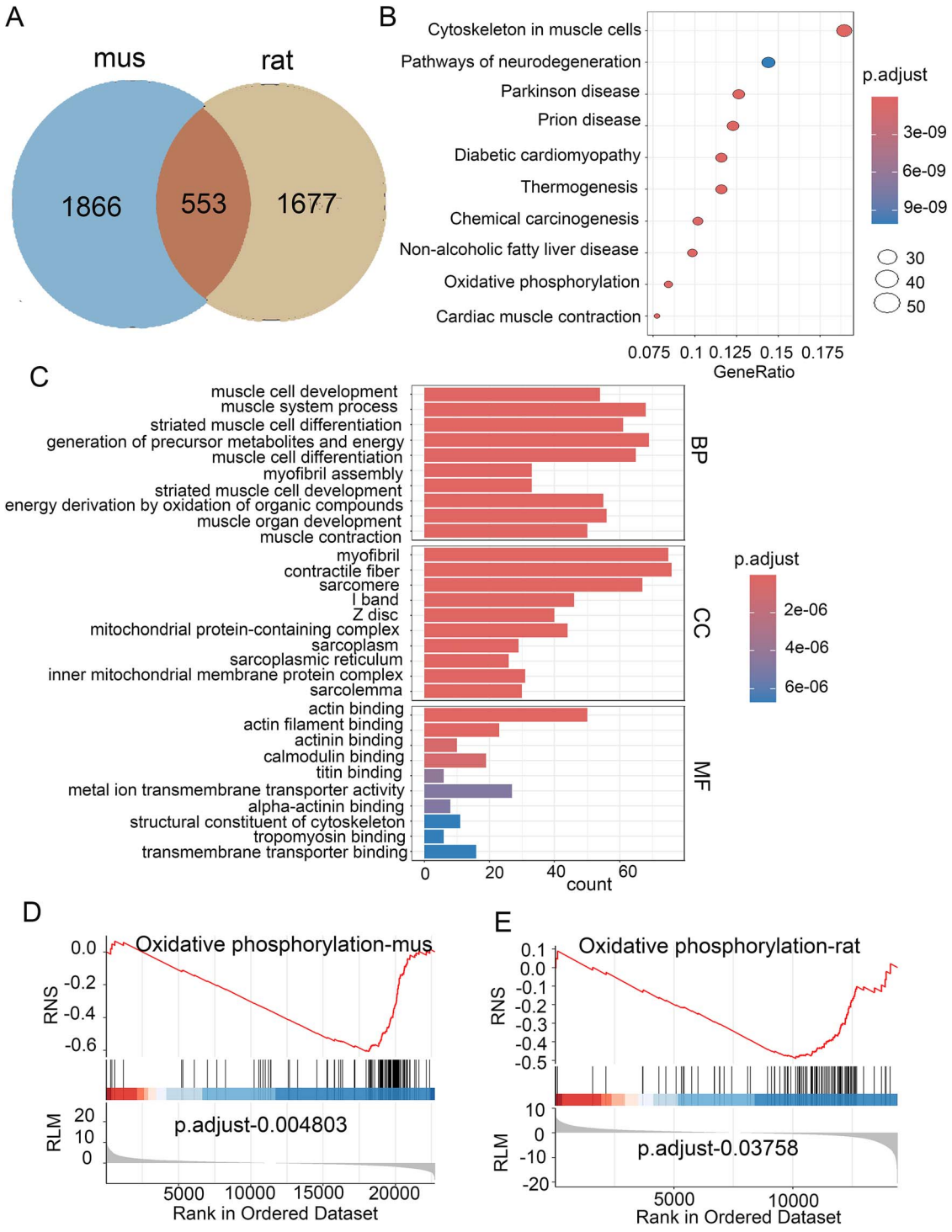

Figure 3. Functional enrichment analysis of homologous down-regulated genes. A. The venn diagram showing the DEGs that are down-regulated in both T2DMED rats and mice. (B) KEGG analysis of co-down-regulated DEGs. (C) GO enrichment analysis of co-down-regulated DEGs. D. GSEA analysis of oxidative phosphorylation pathway in mice. (E) GSEA analysis of oxidative phosphorylation pathway in rats. DEGs: Differentially expressed genes; mus: mouse; KEGG: Kyoto Encyclopedia of Genes and Genomes; GO: Gene Ontology; BP: biological process; MF: molecular function; CC: cellular component; GSEA: gene set enrichment analysis.

DEGs in T2DMED rats and mice

After analyzing DEGs using the DESeq2 package on RNA-seq data from rats and mice, we identified 4820 DEGs in T2DMED mice compared to the normal group, of which 2419 (50.18%) were down-regulated and 2401 (49.82%) were up-regulated (Figure 2A and B). Similarly, in T2DMED rats, 3969 DEGs were identified, with a slightly higher proportion of down-regulated DEGs at 56.18% (2230) compared to the normal group (Figure 2C and D). To explore the biological changes shared between the two species, we identified the intersection of DEGs from both groups, resulting in 1184 homologous DEGs (Figure 2E).

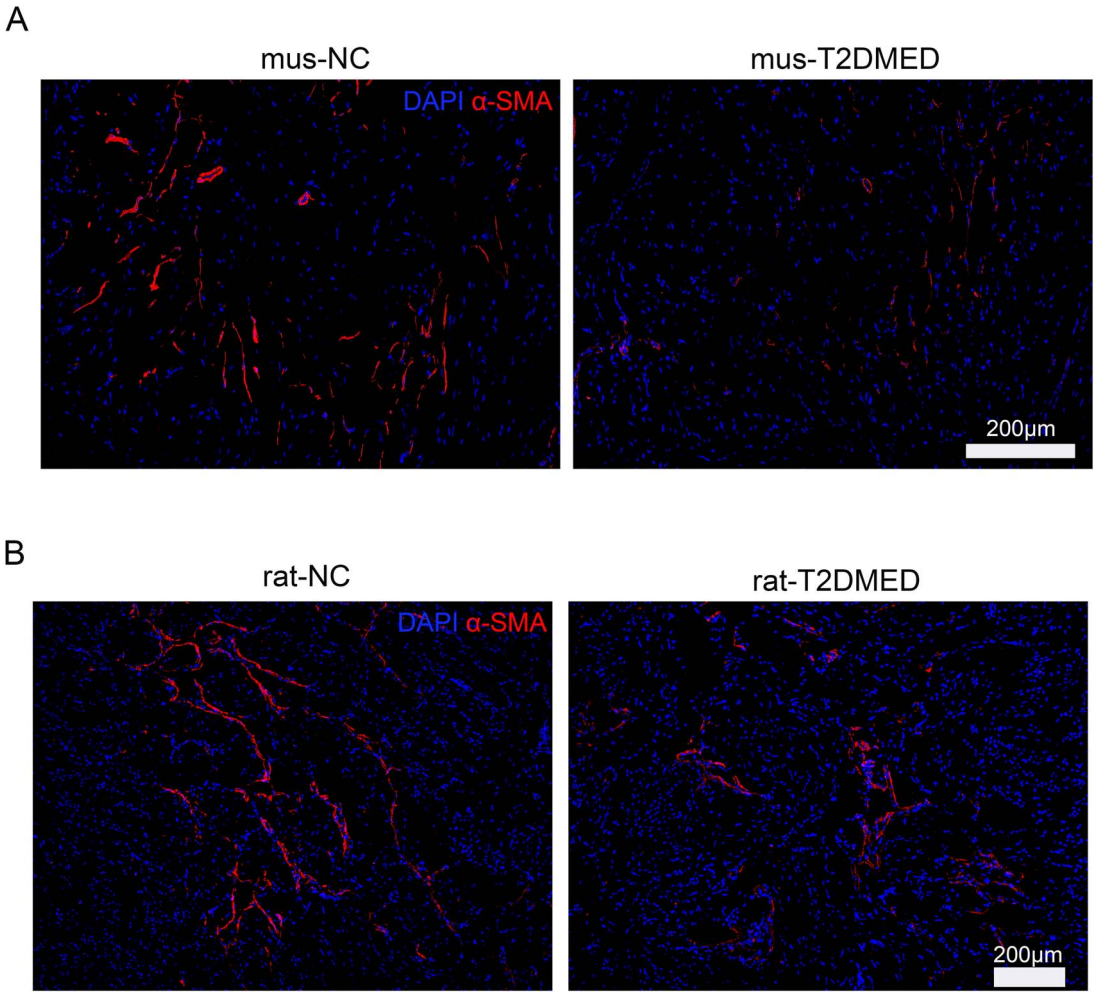

Figure 4. The decreased expression of α-SMA both in T2DMED rats and mice. A. Immunofluorescence staining of α-SMA in the corpus cavernosum of the mice. (200x) B. Immunofluorescence staining of α-SMA in the corpus cavernosum of the rats. mus: mouse; T2DMED: type 2 diabetes-induced erectile dysfunction. (100x).

These homologous DEGs were further classified into four subgroups: the homologous up-regulated group, the homologous down-regulated group, the rat up-regulated but mouse down-regulated group, and the rat down-regulated but mouse up-regulated group. This discrepancy highlights both the similarities and differences between rats and mice in the development of T2DM (Figure 2F). Given that conserved changes across species are more likely to shed light on critical aspects of disease onset and progression, we proposed that the same trend differentially expressed genes (ST-DEGs) might more accurately reflect common biological alterations across species. Therefore, we selected ST-DEGs from both the homologous up-regulated and homologous down-regulated groups for detailed bioinformatics analysis, aiming to uncover key molecular mechanisms and potential therapeutic targets for T2DMED.

Functional enrichment analysis of homologous down-regulated genes

A total of 553 homologous down-regulated DEGs were identified in the subset of T2DMED and normal group between the 2 species (Figure 3A). KEGG enrichment analysis revealed that these genes were significantly enriched in pathways related to the muscle cytoskeleton, neurodegeneration, Parkinson's disease, diabetic cardiomyopathy, and oxidative phosphorylation (Figure 3B). GO enrichment analysis indicated that these genes were primarily involved in BP such as muscle development and function, and energy metabolism. Their MF were associated with myofibers and mitochondria (Figure 3C). Furthermore, GSEA enrichment analysis identified 11 commonly down-regulated pathways in both species (Supplementary Table S1), including those related to altered muscle function and mitochondrial oxidative phosphorylation (Figure 3D and E), reinforcing the crucial role of mitochondrial and smooth muscle alterations in the progression of T2DMED.

To further support the credibility of these bioinformatics results, we performed immunofluorescence analysis on rat and mouse cavernous tissues. The results demonstrated a reduction in α-SMA fluorescence intensity in the T2DMED group, indicating a decrease in smooth muscle content during the course of T2DMED in both species (Figure 4A and B, Supplementary Figure S1A and B).

Identification and validation of mitochondria-related DEGs

To further investigate the mitochondrial alterations associated with T2DMED, we retrieved 1140 mitochondrial genes

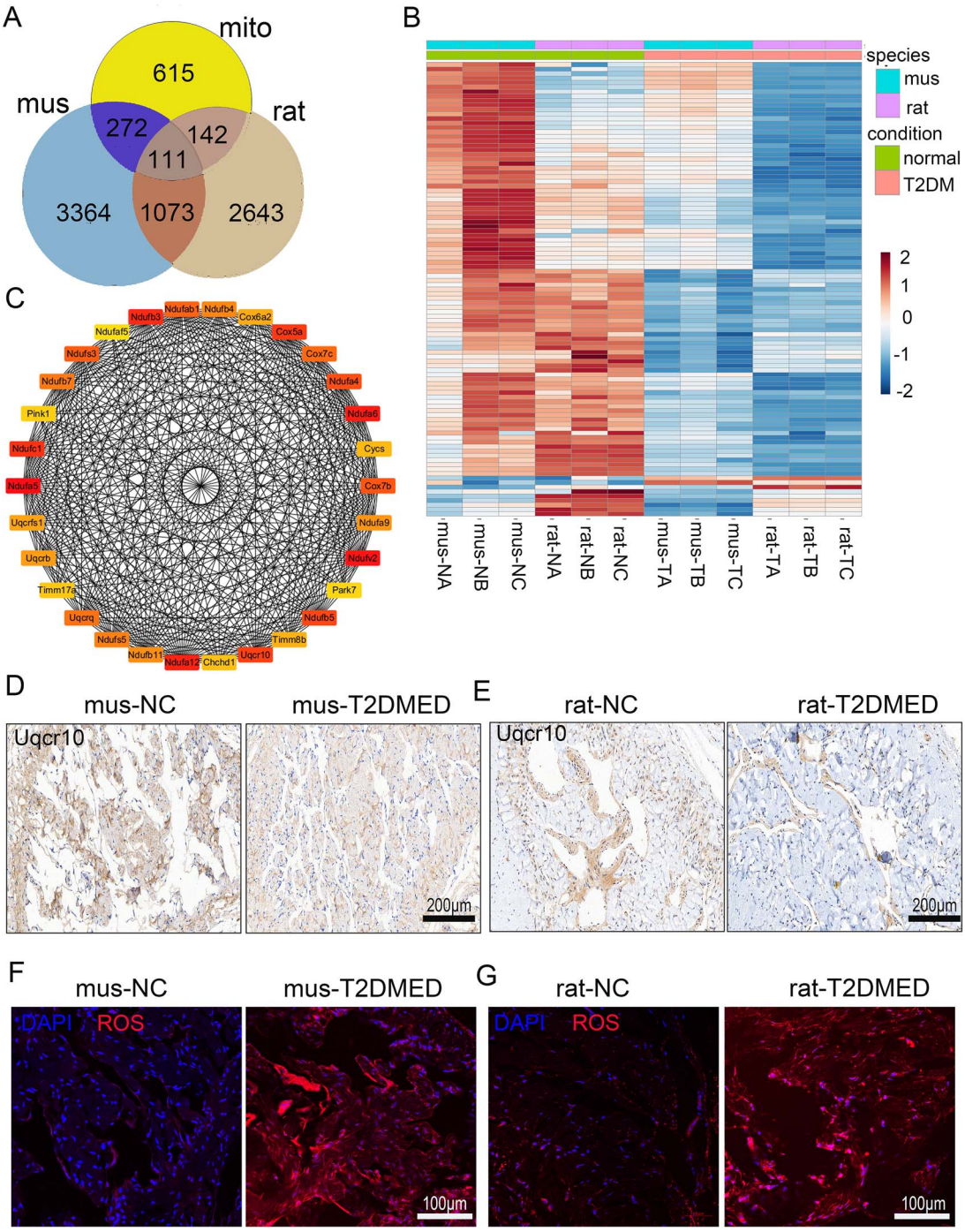

Figure 5. Identification and validation of mitochondria-related DEGs. (A) The venn diagram showing the DEGs among rats, mice and mitochondrial genes. (B) The heatmap showing the hierarchical clustering of common mitochondria-related DEGs in rats and mice. Blue indicates low expression levels and red indicates high expression levels. (C) Interaction network analysis of common mitochondria-related DEGs. (D,E) Immunohistochemical staining of *Uqcr10* in the corpus cavernosum of the mice and rats. (200x) (F-G) The ROS levels in the corpus cavernosum of the mice and rats. DEGs: differentially expressed genes; mus: mouse; T2DMED: type 2 diabetes-induced erectile dysfunction; ROS: reactive oxygen species. (200x).

from the MitoCarta database[26] and compared them with DEGs identified in rats and mice. This analysis revealed 111 mitochondria-related DEGs (Figure 5A), of which 101 were ST-DEGs, and 97 of these ST-DEGs exhibited a down-regulation trend (Figure 5B and Supplementary Table S2).

Using these 101 mitochondrial ST-DEGs, we constructed a PPI network consisting of 91 nodes and 1686 edges. By calculating the NCC, we identified the top 10 hub genes, including *Ndufa5*, *Ndufv2*, *Ndufa6*, *Ndufa12*, *Ndufb3*, *Ndufc1*, *Cox5a*, *Uqcr10*, *Ndufb5*, and *Ndufa4* (Figure 5C). All of these genes are closely linked to mitochondrial function and oxidative phosphorylation processes.

The protein encoded by *Uqcr10* is a key component of mitochondrial respiratory chain complex III, and changes in its expression may indicate mitochondrial dysfunction. Our experimental results showed that the expression of *Uqcr10* was reduced in the T2DM model group (Figure 5D and E). Mitochondria are the primary source of intracellular ROS,

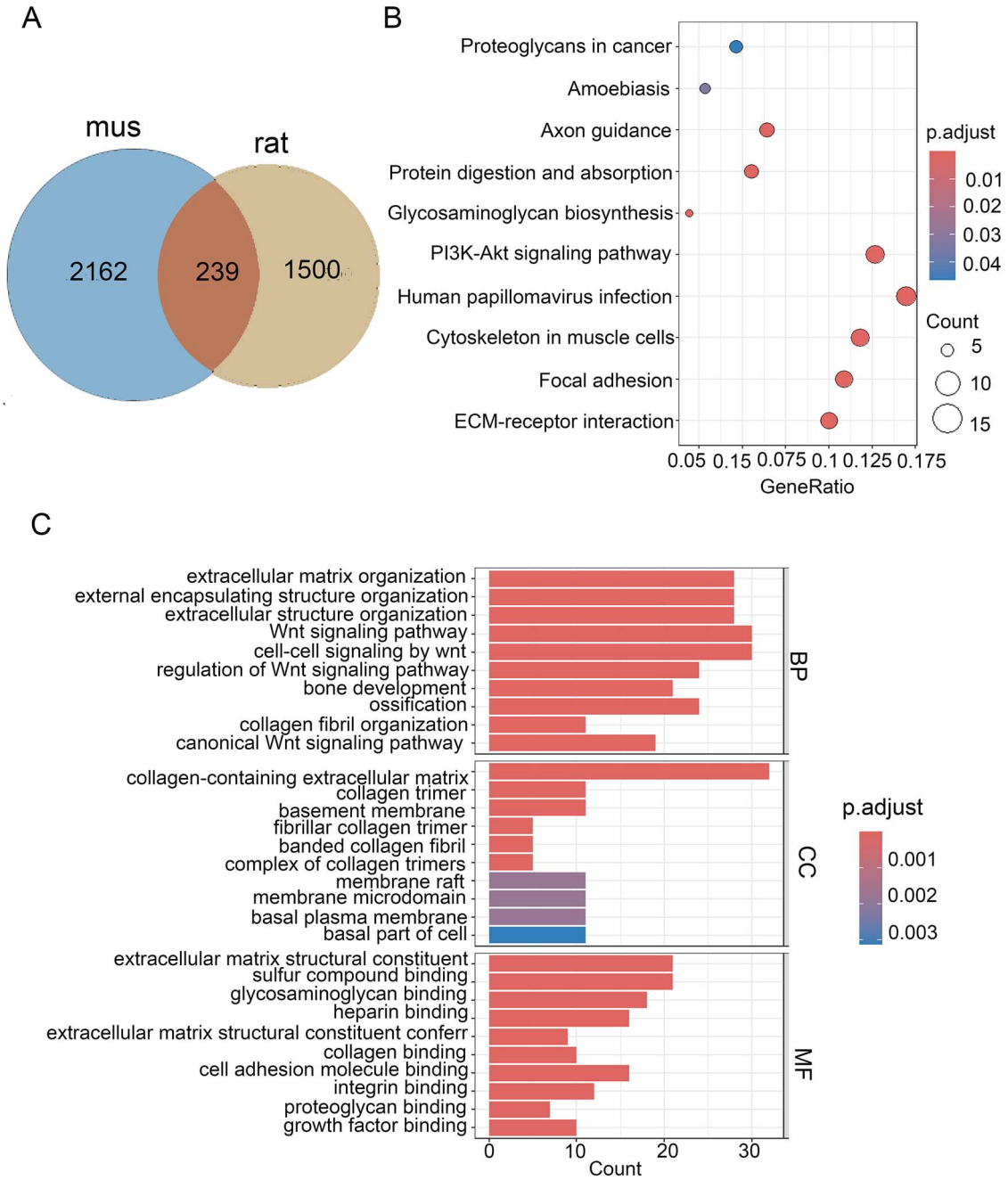

Figure 6. Functional enrichment analysis of homologous up-regulated genes. (A) The venn diagram showing the DEGs that are up-regulated in both T2DMED rats and mice. (B) KEGG analysis of co-up-regulated DEGs. (C) GO enrichment analysis of co-up-regulated DEGs. DEGs: differentially expressed genes; mus: mouse; KEGG: Kyoto Encyclopedia of Genes and Genomes; GO: Gene Ontology; BP: biological process; MF: molecular function; CC: cellular component.

and their dysfunction can lead to abnormalities in the electron transport chain, which subsequently increases ROS production, consistent with what we observed in T2DMED samples (Figure 5F and G). These findings aligned with our bioinformatics analysis, reinforcing that mitochondrial dysfunction may contribute to the progression of T2DMED.

Functional enrichment analysis of homologous up-regulated DEGs

Similarly, we identified 239 co-regulated DEGs among the 1739 up-regulated DEGs in rats and 2401 up-regulated DEGs in mice (Figure 6A). KEGG enrichment analysis of these 239 DEGs revealed that they were primarily enriched in pathways related to the extracellular matrix (ECM), focal adhesion, and proteoglycans (Figure 6B). GO enrichment analysis further indicated that these up-regulated genes involved in BP were associated with the composition of the ECM and *Wnt* signaling pathway. Their CC was predominantly associated with ECM components and membrane structures, with MF related to the recognition, binding of ECM and collagen components (Figure 6C).

In the classical *Wnt* signaling pathway, β-catenin is a key molecule, and changes in its expression levels can reflect the activity of the *Wnt* pathway.[27] The results indicated

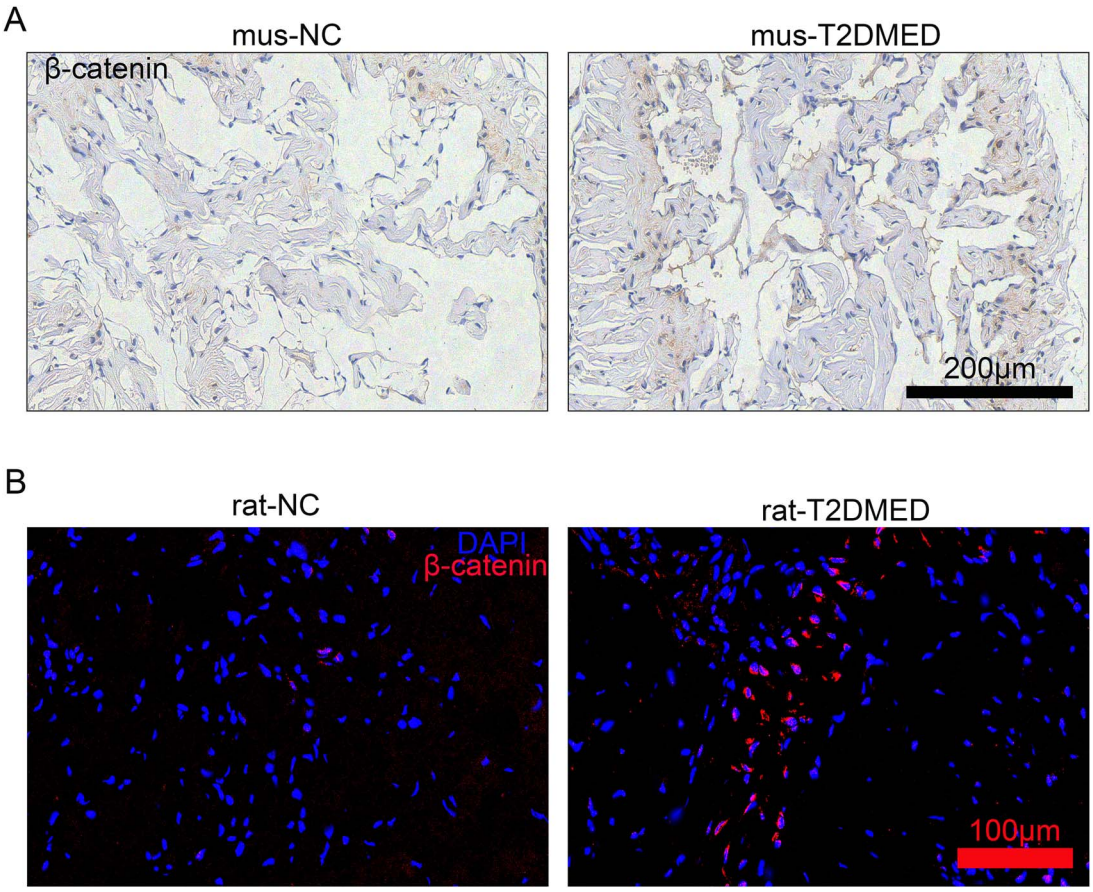

Figure 7. The increased expression of β-catenin both in T2DMED rats and mice. (A) Immunohistochemical staining of β-catenin in the corpus cavernosum of the mice. (300x) (B) Immunofluorescence staining of β-catenin in the corpus cavernosum of the rats. mus: mouse; T2DMED: type 2 diabetes-induced erectile dysfunction. (400x).

that β-catenin expression was significantly elevated in the T2DMED group compared to the normal control group (Figure 7A and B), prompting further investigation into the role of classical *Wnt* signaling pathway in T2DMED.

Analysis and validation of ECM-related DEGs

Based on the results of KEGG and GO enrichment analyses, we hypothesized that the composition of the ECM changes during the progression of T2DMED. To further investigate these changes, we obtained 1105 ECM-related genes from the study by Amelia et al.[28] Intersection analysis of these genes with DEGs identified in rats and mice revealed 120 ECM-associated DEGs (Figure 8A), of which 67 were same-trend DEGs (Figure 8B, Supplementary Table S3). Among these ST-DEGs, the majority (53/67) were up-regulated.

We imported these 67 ST-DEGs into the STRING database to construct a PPI network, consisting of 53 nodes and 554 edges. The top 10 hub genes, based on NCC, included *Col1a1*, *Col1a2*, *Col6a1*, *Col5a1*, *Fbn1*, *Postn*, *Col6a2*, *Col6a3*, *Thbs2*, and *Fn1* (Figure 8C). All of these hub genes were associated with ECM collagen composition, indicating potential alterations in collagen composition within the corpus cavernosum of T2DMED models.

To test this hypothesis, we employed Masson staining, HE staining, and immunohistochemistry to examine the ECM components of the corpus cavernosum in T2DMED rats and mice. The immunohistochemistry results showed upregulation of collagen 1 expression in both T2DMED rats and mice (Figure 8D and E). Additionally, Masson staining and HE staining revealed significant collagen accumulation in the corpus cavernosum of T2DMED groups (Figures 8F-I, Supplementary Figure 1C and D).

Discussion

Cross-species transcriptome not only enhance our understanding of biological system evolution and gene function inference but also help uncover the underlying events of potential diseases.[29] In this study, we performed cross-species transcriptomic comparisons between rats and mice to investigate the fundamental processes involved in T2DMED development. Our results revealed several common molecular features in T2DMED corpus cavernosum across species, highlighting these processes such as down-regulated smooth muscle and mitochondrial functions, up-regulated *Wnt* pathways and ECM composition.

Penile erection is a neurovascular process regulated by psychological and hormonal factors. Sexual stimulation triggers nitric oxide production via neuronal nitric oxide synthase, and activates parasympathetic non-adrenergic, non-cholinergic cavernous nerves, leading to the increased cyclic guanosine monophosphate in cavernous smooth muscle cells. This cascade of signals reduces intracellular calcium ion uptake, promoting relaxation of cavernous smooth

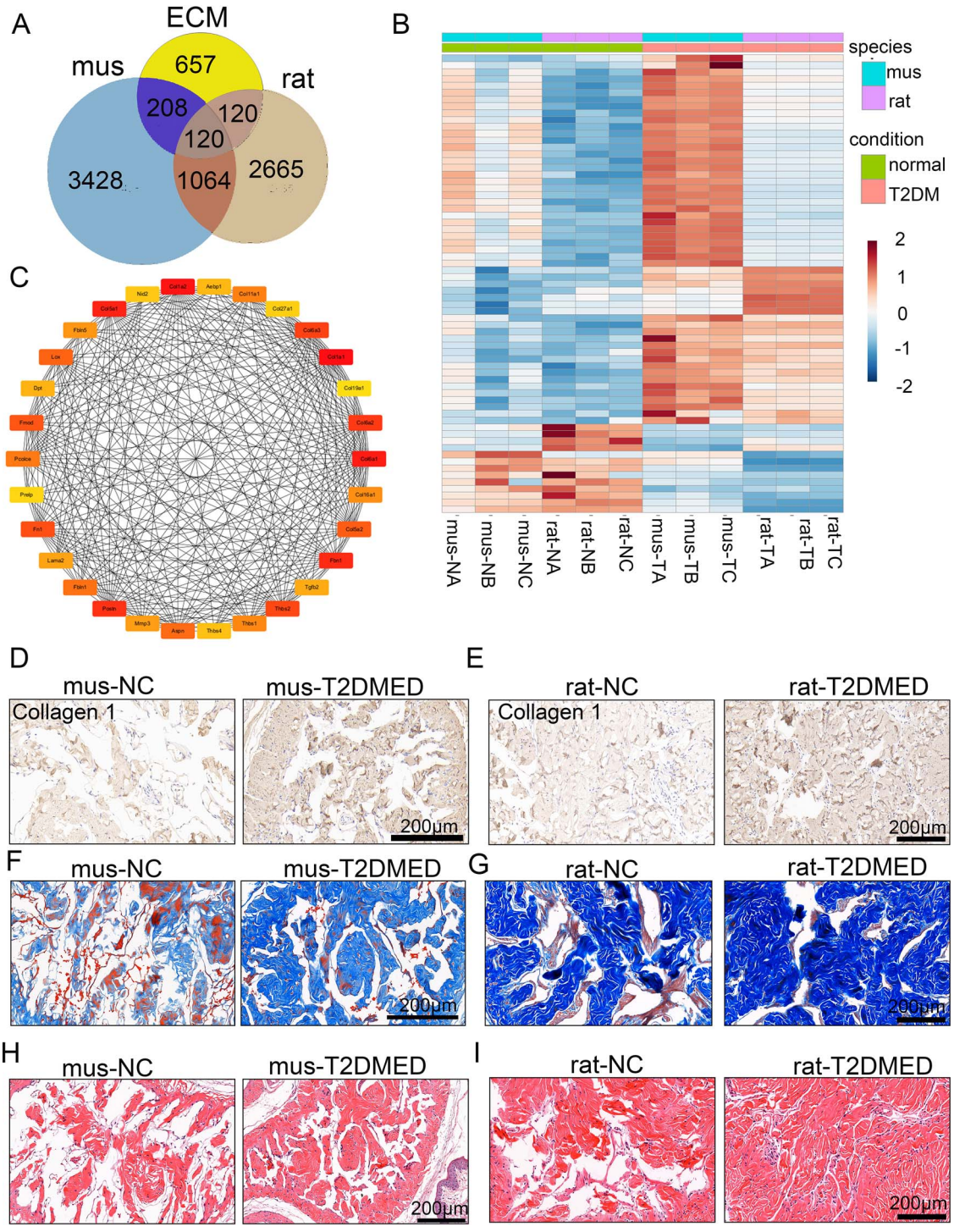

Figure 8. Identification and validation of ECM-related DEGs. (A) The venn diagram showing the DEGs among rats, mice and ECM genes. (B) The heatmap showing the hierarchical clustering of common ECM-related DEGs in rats and mice. (C) Interaction network analysis of common ECM-related DEGs. (D, E) Immunohistochemical staining of collagen 1 in the corpus cavernosum of the mice and rats. (D-300x, E-200x) (F-I) The masson and HE staining in the corpus cavernosum of the mice and rats. DEGs: differentially expressed genes; mus: mouse; T2DMED: type 2 diabetes-induced erectile dysfunction; ECM: extracellular matrix. (F-300x, G-200x, H-200x, I-200x).

muscle cells, dilation of the cavernous sinus, and blood influx.[30] Consequently, the contraction and relaxation of cavernous smooth muscle regulate sinus dilation and penile erection. In previous studies, our team demonstrated that both cisplatin-related and cavernous nerve injury-induced ED rat models exhibited decreased smooth muscle content.[31,32] Transcriptome sequencing of cavernous tissue from T2DM models of various species revealed significant downregulation of smooth muscle-related genes and pathways, indicating that reduced smooth muscle content and function contribute to T2DMED pathogenesis. Prior studies have shown that maintaining normal smooth muscle structure and function can significantly improve erectile function in diabetic rats and mice.[33,34]

Mitochondria are crucial for maintaining cellular homeostasis. They serve as the energy center of all eukaryotic cells by synthesizing adenosine triphosphate via oxidative phosphorylation, while also playing a pivotal role in calcium ion storage, cellular differentiation regulation, and biomolecule synthesis.[35] Mitochondria are semi-autonomous, possessing their own DNA and systems for replication, transcription, and translation. However, mitochondrial DNA is more vulnerable to oxidative damage than nuclear DNA, largely due to its role in generating ROS through the electron transport chain.[36] Mitochondrial dysfunction is closely linked to numerous human diseases, including neurological disorders, cardiovascular diseases, renal dysfunction, and diabetes and its complications.[37]

In previous studies, we have demonstrated that a mechanotherapeutic apparatus can activate mitochondrial autophagy, maintain mitochondrial numbers and function, and reduce ROS production, enhancing cellular tolerance to glycosylation end products.[38] In this study, we identified a general downregulation of mitochondria-related genes in the corpus cavernosum of T2DMED models, suggesting that T2DMED is also a mitochondria-associated disorder. Understanding the regulatory mechanisms of mitochondrial homeostasis may provide deeper insights into T2DMED pathogenesis.

The evolutionarily conserved *Wnt* signaling pathway plays a central role in development and tissue homeostasis across species. *Wnt* proteins are secreted lipid-modified molecules that activate β-catenin-dependent signaling, promoting cell proliferation, differentiation, and maturation.[27] Previous studies have shown increased expression of *Wnt*-related genes in corpus cavernosum of streptozotocin-induced type 1 diabetic mice, including *Wnt3*, *Wnt3a*, *Wnt4*, *Wnt8a*, *Wnt8b*, and *Wnt10b*, compared to controls. Moreover, *Wnt* antagonists have been shown to enhance penile angiogenesis, nerve regeneration, and improve erectile function in diabetic mice.[39] Similarly, in our study, we observed abnormal activation of the *Wnt* signaling pathway in the cavernous tissues of T2DMED rats and mice, indicating that further elucidation of key *Wnt* molecules may develop new therapeutic avenues for DMED.

The ECM is a complex accumulation of structural and functional molecules secreted by cells and is a major component of the extracellular environment.[40] The shape and function of fibroblasts in corpus cavernosum are influenced by ECM stiffness. Fibroblasts in soft environments are round, but as ECM stiffness increases, they elongate and form spindle shapes, while neutral lipids and cholesterol levels decrease.[41] Cavernous fibrosis is a key factor in refractory ED, and collagen aggregation and increased ECM content have been observed in the cavernous tissues of patients with vasogenic ED and diabetic rats.[42,43] Our study identified ECM composition alterations as a pathological feature of T2DMED cavernous tissues. Recent advances in understanding how cells sense and regulate ECM mechanical properties highlight the role of components such as elastin, collagen, integrins, and vinculin.[44] Cells maintain tissue integrity and function by sensing and regulating ECM properties, and loss of this regulation may lead to pathological changes. Understanding the molecular mechanisms that control ECM interactions may be essential for developing therapeutic strategies for T2DMED.

This study has several limitations. First, despite the high degree of homology between rats and mice, there are still differences in gene expression patterns, behavior, and cognition. Second, we explored common molecular changes in the corpus cavernosum of T2DMED rats and mice, but further validation is required to determine whether these processes are conserved in human T2DMED tissues. Third, by focusing only on changes shared between the species, we may have overlooked important molecular features specific to either T2DMED rats or mice. Finally, although we have listed several common changes between the DMED rats and mice, there are still many important genes or pathways that need to be further explored and validated.

Conclusions

The lack of effective clinical treatments has driven intensive research into innovative therapies for T2DMED. Cross-species transcriptomic comparisons may offer a novel strategy for uncovering the underlying mechanisms and identifying therapeutic targets for T2DMED.

Acknowledgments

We would like to thank Ms. Chen Ying for her experimental guidance.

Author contributions

Yuxin Tang conceived this study; Ming Xiao designed the methods; Ming Xiao and Huanqin Zeng performed the majority of experiments and analyzed the data; Xiaoli Tan and Ming Xiao constructed the rat model of type 2 diabetes. Yanghua Xu and Jiarong Xu designed the experimental procedures; Ming Xiao and Huanqin Zeng wrote the original manuscript; Yuxin Tang reviewed and edited the manuscript. All authors have read and approved the final version of the manuscript. Ming Xiao and Huanqing Zeng contributed equally.

Supplementary material

Supplementary material is available at *Sexual Medicine* online.

Funding

This study was supported by the Guangdong Basic and Applied Basic Research Foundation (2024A1515013146, Y.X.T.) and the National Natural Science Foundation of China (82371632, Y.X.T.).

Conflicts of interest

The authors have declared that no competing interest exists.

Data availability

The data used to support the findings of the present study are available from the corresponding author upon request.

References

1. Ayta IA, McKinlay JB, Krane RJ. The likely worldwide increase in erectile dysfunction between 1995 and 2025 and some possible policy consequences. *BJU Int*. 1999;**84**(1):50–56. https://doi.org/10.1046/j.1464-410x.1999.00142.x
2. Shiferaw WS, Akalu TY, Petrucka PM, Areri HA, Aynalem YA. Risk factors of erectile dysfunction among diabetes patients in Africa: a systematic review and meta-analysis. *J Clin Transl Endocrinol*. 2020;**21**(3):100232. https://doi.org/10.1016/j.jcte.2020.100232

3. Gatti A, Mandosi E, Fallarino M, *et al.* Metabolic syndrome and erectile dysfunction among obese non-diabetic subjects. *J Endocrinol Investig*. 2009;**32**(6):542–545. https://doi.org/10.1007/bf03346504
4. Sun H, Saeedi P, Karuranga S, *et al.* IDF diabetes atlas: global, regional and country-level diabetes prevalence estimates for 2021 and projections for 2045. *Diabetes Res Clin Pract*. 2022;**183**:109119. https://doi.org/10.1016/j.diabres.2021.109119
5. Thorve VS, Kshirsagar AD, Vyawahare NS, Joshi VS, Ingale KG, Mohite RJ. Diabetes-induced erectile dysfunction: epidemiology, pathophysiology and management. *J Diabetes Complicat*. 2011;**25**(2):129–136. https://doi.org/10.1016/j.jdiacomp.2010.03.003
6. Kumar R, Kumar U, Trivedi S. Comparison of risk factors for erectile dysfunction (ED) in type 2 diabetics and nondiabetics: a retrospective observational study. *Cureus*. 2023;**15**(9):e44576. https://doi.org/10.7759/cureus.44576
7. Zhou F, Hui Y, Xu Y, *et al.* Effects of adipose-derived stem cells plus insulin on erectile function in streptozotocin-induced diabetic rats. *Int Urol Nephrol*. 2016;**48**(5):657–669. https://doi.org/10.1007/s11255-016-1221-3
8. Penson DF, Latini DM, Lubeck DP, *et al.* Do impotent men with diabetes have more severe erectile dysfunction and worse quality of life than the general population of impotent patients? Results from the exploratory comprehensive evaluation of erectile dysfunction (ExCEED) database. *Diabetes Care*. 2003;**26**(4):1093–1099. https://doi.org/10.2337/diacare.26.4.1093
9. Hatzimouratidis K, Hatzichristou DG. A comparative review of the options for treatment of erectile dysfunction: which treatment for which patient? *Drugs*. 2005;**65**(12):1621–1650. https://doi.org/10.2165/00003495-200565120-00003
10. Pajovic B, Dimitrovski A, Fatic N, Malidzan M, Vukovic M. Vacuum erection device in treatment of organic erectile dysfunction and penile vascular differences between patients with DM type I and DM type II. *Aging Male*. 2017;**20**(1):49–53. https://doi.org/10.1080/13685538.2016.1230601
11. Martignoni M, Groothuis GM, de Kanter R. Species differences between mouse, rat, dog, monkey and human CYP-mediated drug metabolism, inhibition and induction. *Expert Opin Drug Metab Toxicol*. 2006;**2**(6):875–894. https://doi.org/10.1517/17425255.2.6.875
12. Yang MS, Xu XJ, Zhang B, Niu F, Liu BY. Comparative transcriptomic analysis of rat versus mouse cerebral cortex after traumatic brain injury. *Neural Regen Res*. 2021;**16**(7):1235–1243. https://doi.org/10.4103/1673-5374.301028
13. Li H, Wang X, Wang Y, *et al.* Cross-species single-cell transcriptomic analysis reveals divergence of cell composition and functions in mammalian ileum epithelium. *Cell Regen*. 2022;**11**(1):19. https://doi.org/10.1186/s13619-022-00118-7
14. Qi Y, Chen Z, Guo B, *et al.* Speckle-tracking echocardiography provides sensitive measurements of subtle early alterations associated with cardiac dysfunction in T2DM rats. *BMC Cardiovasc Disord*. 2023;**23**(1):266. https://doi.org/10.1186/s12872-023-03239-2
15. Yeo HJ, Shin MJ, Yoo KY, Jung BH, Eum WS, Choi SY. Tat-CIAPIN1 prevents pancreatic β-cell death in hIAPP-induced RINm5F cells and T2DM animal model. *Int J Mol Sci*. 2023;**24**(13):10478. https://doi.org/10.3390/ijms241310478
16. Ginestet C. ggplot2: elegant graphics for data analysis. *J R Stat Soc*. 2011;**174**(1):245–246. https://doi.org/10.1111/j.1467-985X.2010.00676_9.x
17. Abdelmoez AM, Sardón Puig L, Smith JAB, *et al.* Comparative profiling of skeletal muscle models reveals heterogeneity of transcriptome and metabolism. *Am J Physiol Cell Physiol*. 2020;**318**(3):C615–C626. https://doi.org/10.1152/ajpcell.00540.2019
18. Love MI, Huber W, Anders S. Moderated estimation of fold change and dispersion for RNA-seq data with DESeq2. *Genome Biol*. 2014;**15**(12):550. https://doi.org/10.1186/s13059-014-0550-8
19. Yu G, Wang LG, Han Y, He QY. clusterProfiler: an R package for comparing biological themes among gene clusters. *OMICS*. 2012;**16**(5):284–287. https://doi.org/10.1089/omi.2011.0118
20. Kanehisa M, Furumichi M, Sato Y, Ishiguro-Watanabe M, Tanabe M. KEGG: integrating viruses and cellular organisms. *Nucleic Acids Res*. 2021;**49**(D1):D545–d551. https://doi.org/10.1093/nar/gkaa970
21. Gene Ontology Consortium. The gene ontology resource: enriching a GOld mine. *Nucleic Acids Res*. 2021;**49**(D1):D325–d334. https://doi.org/10.1093/nar/gkaa1113
22. Liberzon A, Subramanian A, Pinchback R, Thorvaldsdóttir H, Tamayo P, Mesirov JP. Molecular signatures database (MSigDB) 3.0. *Bioinformatics*. 2011;**27**(12):1739–1740. https://doi.org/10.1093/bioinformatics/btr260
23. Szklarczyk D, Gable AL, Lyon D, *et al.* STRING v11: protein-protein association networks with increased coverage, supporting functional discovery in genome-wide experimental datasets. *Nucleic Acids Res*. 2019;**47**(D1):D607–d613. https://doi.org/10.1093/nar/gky1131
24. Su G, Morris JH, Demchak B, Bader GD. Biological network exploration with Cytoscape 3. *Curr Protoc Bioinformatics*. 2014;**47**(1):8.13.1–8.1324. https://doi.org/10.1002/0471250953.bi0813s47
25. Chin CH, Chen SH, Wu HH, Ho CW, Ko MT, Lin CY. cytoHubba: identifying hub objects and sub-networks from complex interactome. *BMC Syst Biol*. 2014;**8**(S4):S11. https://doi.org/10.1186/1752-0509-8-s4-s11
26. Rath S, Sharma R, Gupta R, *et al.* MitoCarta3.0: an updated mitochondrial proteome now with sub-organelle localization and pathway annotations. *Nucleic Acids Res*. 2021;**49**(D1):D1541–d1547. https://doi.org/10.1093/nar/gkaa1011
27. Yu M, Qin K, Fan J, *et al.* The evolving roles of Wnt signaling in stem cell proliferation and differentiation, the development of human diseases, and therapeutic opportunities. *Genes Dis*. 2024;**11**(3):101026. https://doi.org/10.1016/j.gendis.2023.04.042
28. Parker AL, Bowman E, Zingone A, *et al.* Extracellular matrix profiles determine risk and prognosis of the squamous cell carcinoma subtype of non-small cell lung carcinoma. *Genome Med*. 2022;**14**(1):126. https://doi.org/10.1186/s13073-022-01127-6
29. Gerstein MB, Rozowsky J, Yan KK, *et al.* Comparative analysis of the transcriptome across distant species. *Nature*. 2014;**512**(7515):445–448. https://doi.org/10.1038/nature13424
30. Hedlund P, Aszodi A, Pfeifer A, *et al.* Erectile dysfunction in cyclic GMP-dependent kinase I-deficient mice. *Proc Natl Acad Sci USA*. 2000;**97**(5):2349–2354. https://doi.org/10.1073/pnas.030419997
31. Yin Y, Zhou Y, Zhou J, *et al.* Cisplatin causes erectile dysfunction by decreasing endothelial and smooth muscle content and inducing cavernosal nerve senescence in rats. *Front Endocrinol (Lausanne)*. 2023;**14**:1096723. https://doi.org/10.3389/fendo.2023.1096723
32. Ye K, Li Z, Yin Y, *et al.* LIPUS-SCs-Exo promotes peripheral nerve regeneration in cavernous nerve crush injury-induced ED rats via PI3K/Akt/FoxO signaling pathway. *CNS Neurosci Ther*. 2023;**29**(11):3239–3258. https://doi.org/10.1111/cns.14256
33. Xu W, Sun T, Wang J, *et al.* Ferroptosis is involved in corpus cavernosum smooth muscle cells impairment in diabetes mellitus-induced erectile dysfunction. *Andrology*. 2023;**11**(2):332–343. https://doi.org/10.1111/andr.13291
34. Chen K, Huang B, Feng J, *et al.* Nesfatin-1 regulates the phenotype transition of cavernous smooth muscle cells by activating PI3K/AKT/mTOR signaling pathway to improve diabetic erectile dysfunction. *Heliyon*. 2024;**10**(13):e32524. https://doi.org/10.1016/j.heliyon.2024.e32524
35. Li X, Jiang O, Chen M, Wang S. Mitochondrial homeostasis: shaping health and disease. *Curr Med*. 2024;**3**(1):5. https://doi.org/10.1007/s44194-024-00032-x
36. Huang Z, Chen Y, Zhang Y. Mitochondrial reactive oxygen species cause major oxidative mitochondrial DNA damages and repair pathways. *J Biosci*. 2020;**45**(1):84. https://doi.org/10.1007/s12038-020-00055-0
37. Suomalainen A, Nunnari J. Mitochondria at the crossroads of health and disease. *Cell*. 2024;**187**(11):2601–2627. https://doi.org/10.1016/j.cell.2024.04.037

38. Chen Y, Xiao M, Zhao L, *et al*. Low-intensity pulsed ultrasound counteracts advanced glycation end products-induced corpus Cavernosal endothelial cell dysfunction via activating Mitophagy. *Int J Mol Sci*. 2022;**23**(23):14887. https://doi.org/10.3390/ijms232314887
39. Shin SH, Kim WJ, Choi MJ, *et al*. Aberrant expression of Wnt family contributes to the pathogenesis of diabetes-induced erectile dysfunction. *Andrology*. 2014;**2**(1):107–116. https://doi.org/10.1111/j.2047-2927.2013.00162.x
40. Hussey GS, Keane TJ, Badylak SF. The extracellular matrix of the gastrointestinal tract: a regenerative medicine platform. *Nat Rev Gastroenterol Hepatol*. 2017;**14**(9):540–552. https://doi.org/10.1038/nrgastro.2017.76
41. Yin Y, Chen Y, Xu J, *et al*. Molecular and spatial signatures of human and rat corpus cavernosum physiopathological processes at single-cell resolution. *Cell Rep*. 2024;**43**(9):114760. https://doi.org/10.1016/j.celrep.2024.114760
42. Ryu JK, Han JY, Chu YC, *et al*. Expression of cavernous transforming growth factor-beta1 and its type II receptor in patients with erectile dysfunction. *Int J Androl*. 2004;**27**(1):42–49. https://doi.org/10.1046/j.0105-6263.2003.00447.x
43. Zhang LW, Piao S, Choi MJ, *et al*. Role of increased penile expression of transforming growth factor-beta1 and activation of the Smad signaling pathway in erectile dysfunction in streptozotocin-induced diabetic rats. *J Sex Med*. 2008;**5**(10):2318–2329. https://doi.org/10.1111/j.1743-6109.2008.00977.x
44. Humphrey JD, Dufresne ER, Schwartz MA. Mechanotransduction and extracellular matrix homeostasis. *Nat Rev Mol Cell Biol*. 2014;**15**(12):802–812. https://doi.org/10.1038/nrm3896

Sexual Medicine, 2025, 13, qfaf007
https://doi.org/10.1093/sexmed/qfaf007
Original Research